

## Advection schemes and grid design (\*)

M. SCLAVO and L. CAVALERI

*Istituto Studio Dinamica Grandi Masse - S. Polo 1364, 30125 Venezia, Italy*

(ricevuto il 29 Luglio 1997; revisionato il 14 Dicembre 1998; approvato il 29 Gennaio 1999)

**Summary.** — We discuss the characteristics of the first order advection scheme in coastal areas. In particular we focus our attention on the relationship between the geometry of the coast, as represented in the computational grid, and the wave fields derived from a numerical model. Having considered an alternative scheme, we show how the results may depend substantially on the characteristics of the scheme. It follows that, when modelling in coastal areas, the grid distribution and the advection scheme should be chosen taking reciprocal account of their characteristics.

PACS 92.60.Gn – Winds and their effects.

### 1. – Introduction

Wave modelling is widely used for evaluating the wave conditions in a given area. Models are used to forecast future wave conditions and to study the physics of past events. A state of the art discussion is given by Komen *et al.* (1994). Recently, the reliability and the resolution of global wave models have been greatly improved, and they have been adapted for use in coastal areas (see, *e.g.*, Luo and Scavo, 1997). Meanwhile, new models have been developed for the near-shore zone (see, *e.g.*, Ris *et al.*, 1994 and Ris, 1997). The results of such models, when run in areas with complex coastal features, are particularly sensitive to the sea-land contour representation on the computational grid. Hence the subject deserves further consideration.

In wave modelling the equations that represent the physics of the relevant phenomena are solved on a more or less regular grid using various numerical techniques. The computation is split into two parts, dealing, respectively, with the advection of energy across the grid and with the energy exchange from different processes. The purpose of this paper is to examine the relation between the advection scheme and the grid design.

In a spectral wave model the two-dimensional distribution of wave energy in frequency and direction is discretized into  $n$  frequencies and  $m$  directional components. The energy of each component varies over the grid and with time, so the energy density is a dependent function of five variables: frequency, direction, two

---

(\*) The authors of this paper have agreed to not receive the proofs for correction.

spatial co-ordinates and time. We represent this (commonly referred to as the two-dimensional wave spectrum) as  $F(f, \theta, x, y, t)$ .

The sum of the energy present in each of the  $n \cdot m$  components provides the overall energy  $E$ , which is related to the significant wave height  $H_s$ . Different weighted sums provide other relevant parameters, such as the mean frequency  $f_m$  and the mean direction  $\theta_m$ .

At each time step the energy in each component is advected in the direction  $\theta$  with a group velocity  $c_g$  which depends on the frequency  $f$ . In deep water  $c_g = g/4\pi f$ , where  $g$  is the gravitational acceleration. In shallow water the group velocity is also dependent on the water depth.

Many numerical schemes have been developed for the advection process. The most popular one in wave modelling is the first order upwind scheme. The scheme is very simple (a short description is given in the next section) and, because of that, it has some drawbacks, the most notable one being its high rate of dispersion. Truly enough, higher order schemes have been used. However, the first order upwind one is still the most popular one, as a very good compromise between physics of the waves, numerical characteristics, computational time and accuracy. The first order upwind scheme is implemented in the WAM model (WAMDI, 1988; Komen *et al.*, 1994), used by most major meteorological and oceanographic centers in the world for daily forecast and hindcast of the past storms. While studying the characteristics of the scheme close to the coast (Cavaleri and Sclavo, 1998) we realized their close relationship with the way the coastal profile is represented into the grid. We realized also that in certain conditions the scheme is unable to reproduce the physical truth. This led us to develop a modified version of the scheme, with better performances, particularly in coastal waters. A full discussion of the subject is given in the above paper.

For our present purposes the main point is that the same geometry of the grid could be differently interpreted, depending on which advection scheme was used. This was the stimulus for a series of tests aiming at clarifying the problem. In this paper we summarize our findings and draw our conclusions.

We wish to point out that the results of the tests are not strictly related to the order of the scheme. We are obviously fully aware that many more sophisticated numerics are regularly used. However, the characteristic of the scheme that matters for our discussion is its capability to advect not only along two orthogonal directions, but also along the diagonal. The first order upwind and its modified version should therefore be conceived as suitable tools for exploring the implications of the above-mentioned differences. As such, our results are potentially valid also for at least some of the more complicated schemes.

The paper is organized as follows. In sect. 2 we briefly describe the two advection schemes. Then, in sect. 3, we describe the various cases considered for the test. The results, together with the related explanations, are given in sect. 4. Finally, sect. 5 provides our conclusions.

## 2. – Advection scheme

The geometrical interpretation of the first order upwind advection scheme is given in fig. 1a, where  $ABCD$  represents one grid mesh.

The energy in  $A$  at time  $t$  is advected to  $P$  after  $\Delta t$ , with  $AP = c_g \Delta t$ . The energy is then redistributed throughout points  $A$ ,  $B$  and  $D$ . To achieve this, the vector  $AP$  is split

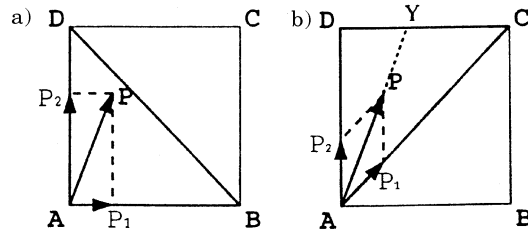


Fig. 1. – Geometrical interpretation of the “quadrant” and “octant” schemes for first order advection. The thicken lines denote the area influenced by one-step advection. a) Quadrant scheme, b) octant scheme.

into its two components  $AP_1$  and  $AP_2$ . Then the energy is redistributed proportionally to the size of the components, leading to

$$E_B^+ = E_A \frac{AP_1}{AB} ; \quad E_D^+ = E_A \frac{AP_2}{AD} ; \quad E_A^+ = E_A - E_B^+ - E_D^+ ,$$

where the superscript + indicates quantities at time  $t + \Delta t$ .

Since we cannot advect away more energy than we have at  $A$ , *i.e.* the energy left at  $A$  at time  $t + \Delta t$  cannot be negative, point  $P$  must be within the heavily bordered area  $ABD$ . The scheme involves the four orthogonal propagation directions, splitting the space in four quadrants, and hereafter we refer to this scheme as  $Q$  (=quadrant).

The point that triggered our interest is that the scheme performs poorly when a wave system is moving along and adjacent to an oblique coast. As shown in fig. 2, the reason is that, to move from  $A$  to  $C$ , the energy must pass through  $B$  and  $D$ . Being  $D$  a land point the energy that ends there is absorbed from the system.

To overcome the problem we proposed the scheme sketched in fig. 1b. Using the same numerical rules as for the upwind scheme, the energy is, in one time step, distributed between  $A$ ,  $C$  and  $D$  rather than  $A$ ,  $B$  and  $D$ . As, in this case, the advection scheme involves eight possible propagation directions (the four cardinal directions plus the four diagonals) and it splits the advection space into eight parts, we refer to this scheme as “octant” ( $O$ ). A similar scheme, named the “angle derivative upstream scheme”, has been used by Tolman (1989, 1991) at the land-sea boundaries of the spatial domain, to ensure correct propagation along a slanting coast.

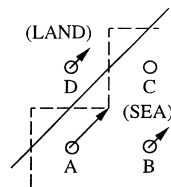


Fig. 2. – Advection from  $A$  to  $C$ , parallel to a slanting coast, implies first the passage of energy through points  $B$  and  $D$ . However, energy at  $D$  (land point) is lost, improperly impoverishing the field energy. The continuous line represents the actual coast, the broken line is its representation in the grid.

For the present discussion, the basic difference between the two schemes is that the Q scheme acts along four directions, while O propagates the energy in four more directions along the diagonals. This is beneficial in areas with a complicated coastal shape and with scattered islands. In the next section the performance of the two schemes is analyzed in different conditions and with several different geometries.

The tests have been carried out using the WAM cycle 4 model, discussed by Komen *et al.* (1994). The model propagates the wave energy by means of a first order upwind advection scheme which, under certain conditions, suffers from the energy loss previously described. For this series of tests, the WAM model is used in a “pure advection” mode. However, the results are applicable for all general cases (most of the following results depend only on the choice of the grid and/or the propagation axes).

As set up for this series of tests, the model advects an energy spectrum  $F(f, \theta, x, y, t)$  across a regular square-mesh grid. The spectrum is discretized into 25 frequencies  $f_i$  ( $i = 1, 25$ ) defined by the rule  $f_i = 0.05 \cdot 1.1^{i-1}$  Hz, and 24 equispaced directions  $\theta_i$  ( $i = 1, 24$ ). We used a  $12 \times 12$  Cartesian grid (with 20 km step size) and a time step of 900 s. All tests were carried out providing the model with a constant boundary input, as specified in the following section.

### 3. – Tests

Apart from the grid geometry, the final results from a given advection scheme depend on the characteristics of the propagated waves. Therefore, we have devised a series of tests in which we systematically varied the following parameters:

– *Coastal shape.* We considered six different patterns, as shown in fig. 3, the circles representing land points. All the tests were carried out in deep water.

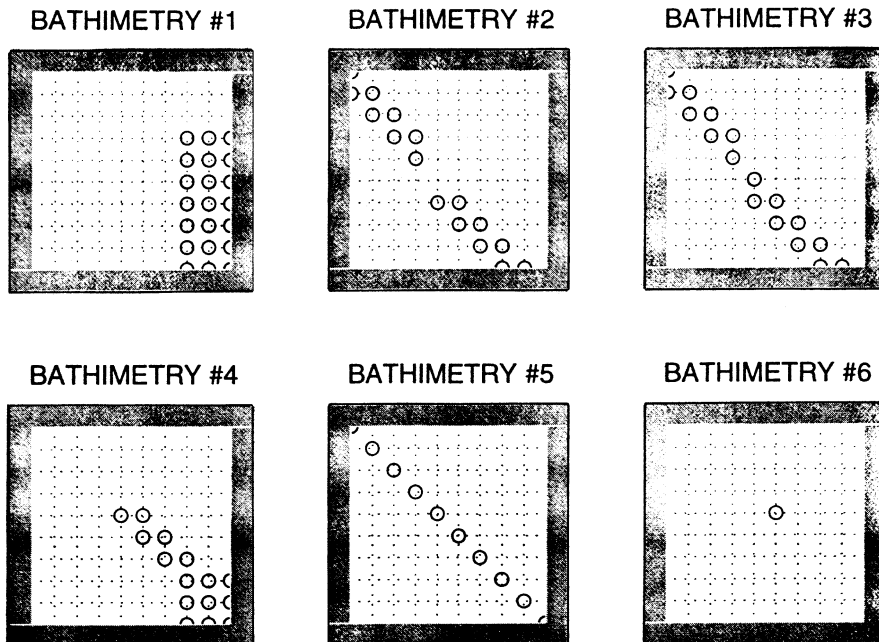


Fig. 3. – The six coastal shapes used in the tests. The circles represent land points.

– *Advection scheme.* We used both the O and the Q schemes described in sect. 2.

– *Wave direction, i.e.* the mean direction along which energy propagates. This is evaluated clockwise from North.

– *Directional resolution, i.e.* the angle between two consecutive directions in the range of  $m$  considered. We used  $m = 12$ , in line with common practice in wave modelling (resolution =  $360^\circ/12 = 30^\circ$ ), or  $m = 24$  ( $15^\circ$ ).

– *Directional shift.* It is common practice to start computing the directions from North and to proceed clockwise, so that the central direction of the first bin corresponds to  $0^\circ$  N, the second to  $(360/m)^\circ$  N and so on. However, this is not strictly necessary and therefore, after using the usual direction setting, we shifted the whole set of values by half the directional resolution ( $15^\circ$  for  $m = 12$  and  $7.5^\circ$  for  $m = 24$ ).

– *Spectral width.* Formally, advection acts on each single-wave component defined in the  $f$ - $\theta$  space. To help understand the investigated numerical features, some tests were carried out using a mono-frequency uni-directional spectrum, which may be considered representative of a single-wave component. In practice real conditions span from highly peaked frequency and direction spectra (swell) to the classical Jonswap spectrum, the latter with a wider frequency distribution. To better show the consequences of advection both these cases have been considered in subsequent tests. For the swell and for the Jonswap spectra a quite sharply peaked directional distribution was assumed.

The overall combinations of tests is summarized in table I. Representative results are presented in the next section.

TABLE I. – *List of tests and acronym meaning.*

		<i>LABEL</i>
<i>Coastal shape</i>	6 patterns	1-6
<i>Advection scheme</i>	quadrant octant	Q O
<i>Wave direction</i>	180° N 210° N 225° N	180 210 225
<i>Directional resolution</i>	30° 15°	12 d 24 d
<i>Directional shift</i>	0° 7.5° 15°	0 s 7.5 s 15 s
<i>Spectral shape</i>	mono-freq./uni-dir. peaked ( $f, \theta$ ) JONSWAP	MON PEA JON

#### 4. – Results

4.1. *Corner of a coast.* – As a first test we consider the corner of a coast (layout 1 in fig. 3).

In fig. 4a and b the incoming wave field is from 45°. The results show clear differences between the O and Q schemes. Advecting along the orthogonal Cartesian directions (in this case W and S), Q extends the wave field in the shadow of the coast. When advecting along a diagonal, O maintains a sharp border between the shadowed zone and the region affected by the wave field. Note how the wave direction is unphysically kept constant in the Q shadow area and how the over-shadowed area

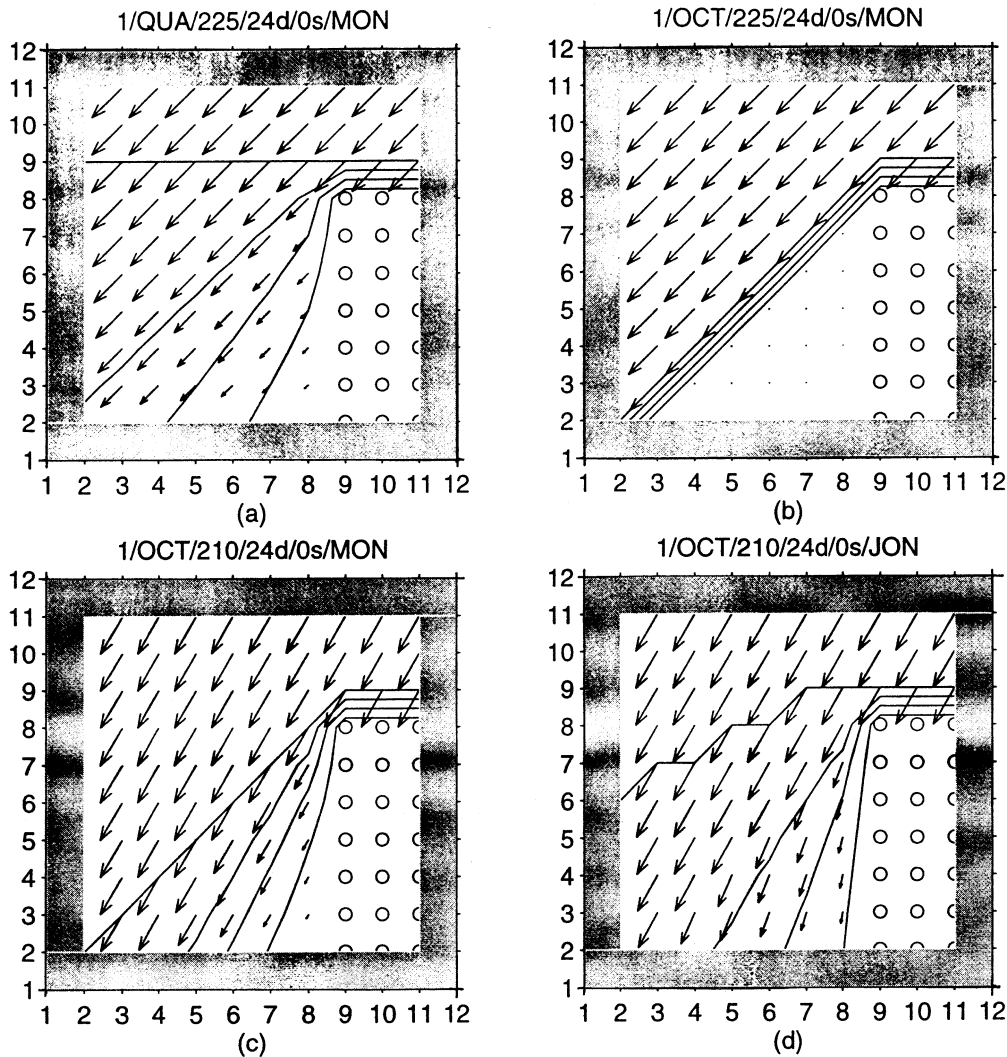


Fig. 4. – Advection around a corner of the coast. See table I for details on the single test. The wave height isolines are spaced at 25% of the undisturbed value. Land points are represented by circles. Both axes are labelled by grid points.

extends horizontally well off the coast (the isolines of the wave height are shown at intervals of 1/4 of the undisturbed value). A small change in the incoming wave direction (4c) causes O to under-shadow the corner area, because now some energy is advected vertically as well as diagonally; nevertheless, the under-shadow effect is less pronounced than with the Q scheme (not shown here). Figure 4d finally shows how the use of a more realistic Jonswap spectrum, with a broader directional distribution, allows a more realistic wave direction in the shadow area and causes a type of numerical “false diffraction”.

4.2. *Two facing oblique peninsulas.* – Figure 5 shows the results of the advection

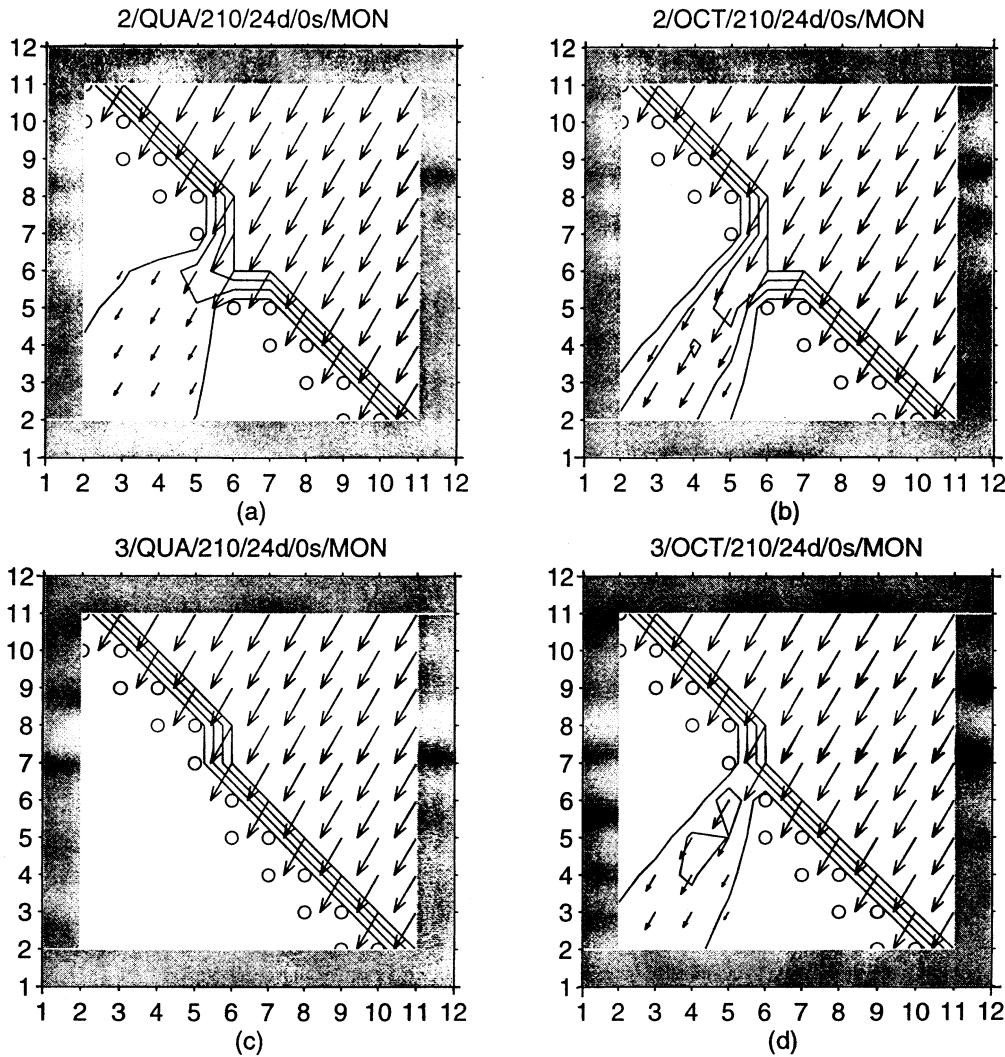


Fig. 5. – Advection across two facing oblique peninsulas. See table I for details on the single test. The wave height isolines are spaced at 25% of the undisturbed value. Land points are represented by circles.

across two facing oblique peninsulas. In panel a) and b) a small gap between two oblique peninsulas has been used (see layout 2 in fig. 3). Note how, with the same input conditions, O allows a much larger energy flow through the gap.

The reason is more evident referring to fig. 3. With scheme Q, energy can flow only horizontally and vertically, with only one possible path through the gap of layout 2. On the contrary, scheme O can move the energy also along the diagonals of the grid mesh, and therefore it can transfer the energy along multiple paths, allowing an increased flow of energy.

Figures 5c and d show a more extreme case, corresponding to geometry 3 of fig. 3. Here a diagonal path is the only possible one. As a consequence, Q “sees” the two peninsulas as a single stretch of land, and no energy can pass. Again, O is still capable of some energy flow through the narrow gap, recognising the geometry as two facing oblique peninsulas.

4.3. *Continuous oblique series of land points.* – Using layout 5 of fig. 3 we can approach the problem from a different perspective, considering what such a coastal configuration actually represents. Two intuitive, but opposite, answers come to the mind: a narrow oblique peninsula or a sequence of islands. Clearly in the former case no energy must flow through, while in the latter some flow must be allowed through the islands. These two interpretations are reflected in the results obtained using Q and O, respectively, as shown in fig. 6a and b.

We want to point out that the results of any propagation scheme applied to straits or narrow gaps must be carefully checked to ensure (using a proper sea/land layout) the energy flux conservation or, at least, to assess the related energy loss. Failing to consider this point may lead to unphysical underestimation of the wave field in the lee of the strait.

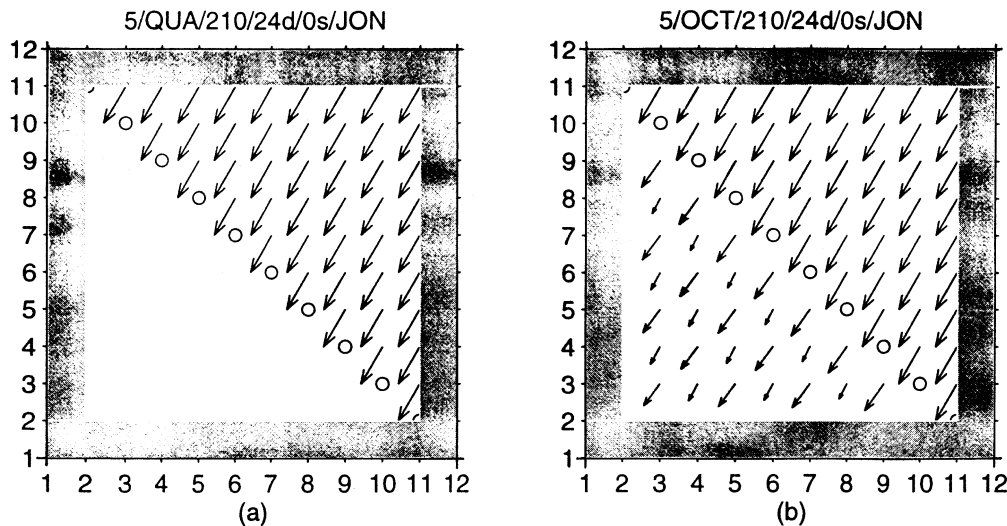


Fig. 6. – Advection across an oblique sequence of land points. a) Q scheme, b) O scheme (see table I for details on the single test). Land points are represented by circles.



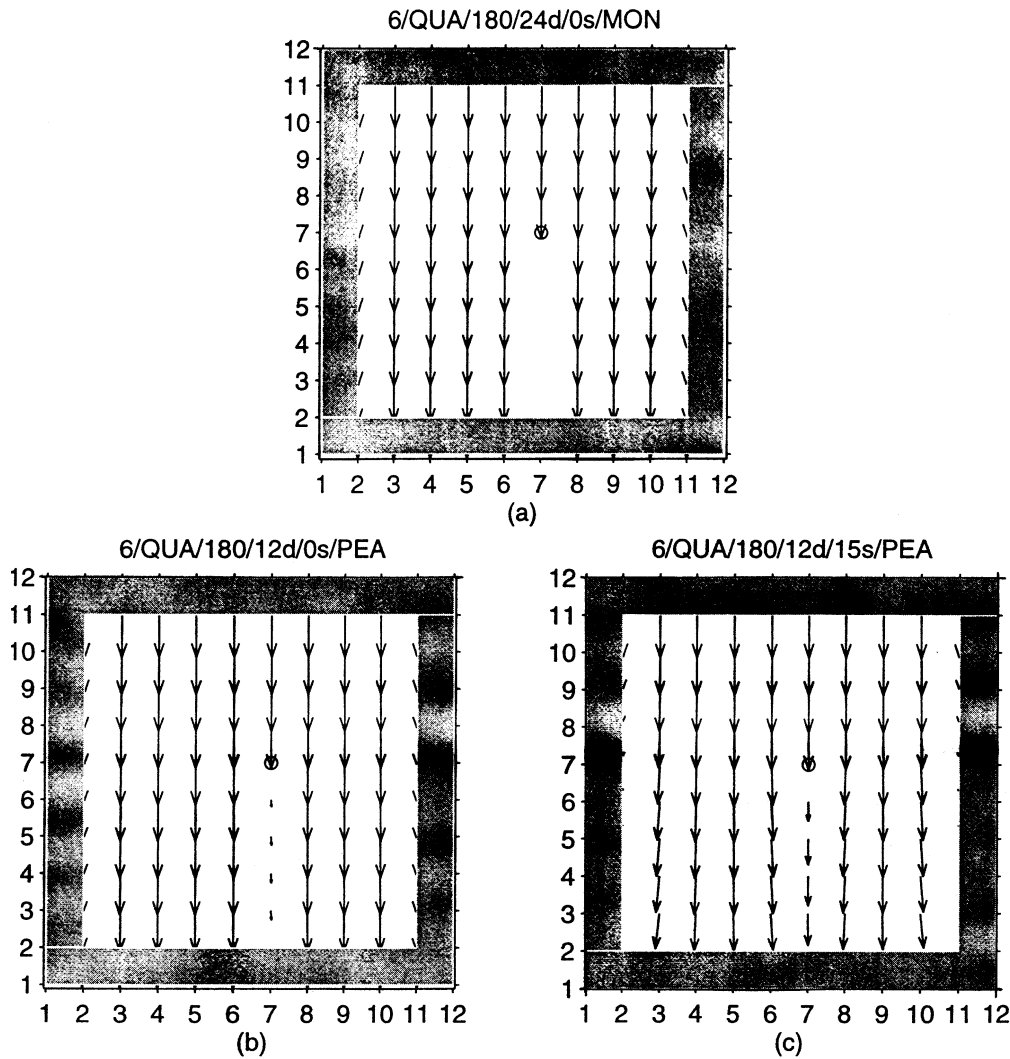


Fig. 7. – Advection past an island, represented by the isolated circle. See table I for details on single test. Both axes are labelled by grid points. a) Mono-frequency, uni-directional spectrum, b) peaked swell, c) as b), but with directional shift.

4.4. *Isolated island.* – Figure 7 shows some results obtained simulating a North to South flow of energy encountering an isolated island (layout 6 in fig. 3). Considering the monochromatic-unidirectional case of fig. 7a, we see that the shadow of the island extends indefinitely. The reason is that when energy propagates along one of the main directions of the advection system, it is propagated only along this direction, with no transverse diffusion. As a consequence, the energy on the sides of the island moves South, without filling the gap in the middle. The result is a shadow extending indefinitely along the field. A good practical example is provided by Bidlot *et al.* (1997).

A frequency-peaked distribution, with a narrow directional distribution, still suffers from the same problem (7b), even if the small oblique lateral components of the spectrum show a tendency to fill the gap slightly. As the results are unrealistic (in nature the shadow, even if long, is limited in space also in case of swell), a solution is provided by a simple numerical fix (suggested by H. Gunther and reported by P. Janssen, personal communication). Figure 8a shows the classical distribution of 12 directions, at 30 degree intervals, starting from North and continuing clockwise. The broken lines show the directions coincident with the advection directions, *i.e.* the directions along which shadowing is possible.

However, there is no need to start from  $0^\circ$ . Rotating the system by half the directional resolution (in this case  $15^\circ$ ), we obtain the distribution sketched in 8b.

With Q no direction is now coincident with the advection direction, hence indefinite shadowing is not possible. The result of the aforementioned direction shift is presented in 7c, where the shadow of the island has more reasonable dimensions. Numerically, the two directions to the right and left of south, along which the flow is concentrated, have an obvious tendency to fill the gap, leading to a qualitatively correct result.

It is interesting to point out that the directional distribution reported in panel 8b is not a solution for the O scheme, because in this case the advection directions (broken lines) coincide with angles which are centres of directional bins ( $45^\circ$ ,  $135^\circ$ ,  $225^\circ$ ,  $315^\circ$ ).

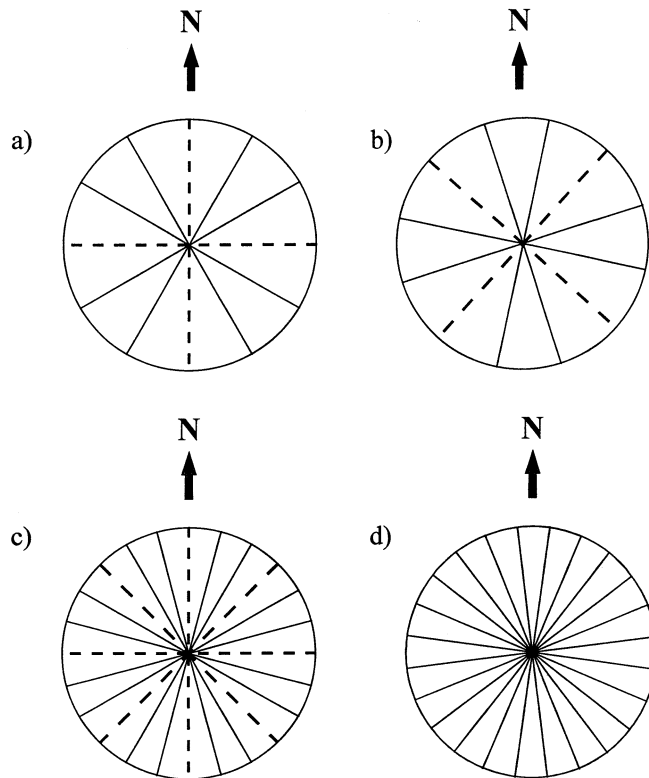


Fig. 8. – The directional distribution considered in the wave model. a) 12 directions; b) as a), but shifted of  $15^\circ$ ; c) 24 directions; d) as c), but shifted of  $7.5^\circ$ . The broken lines in panels a, b and c show the directions along which shadowing is possible.

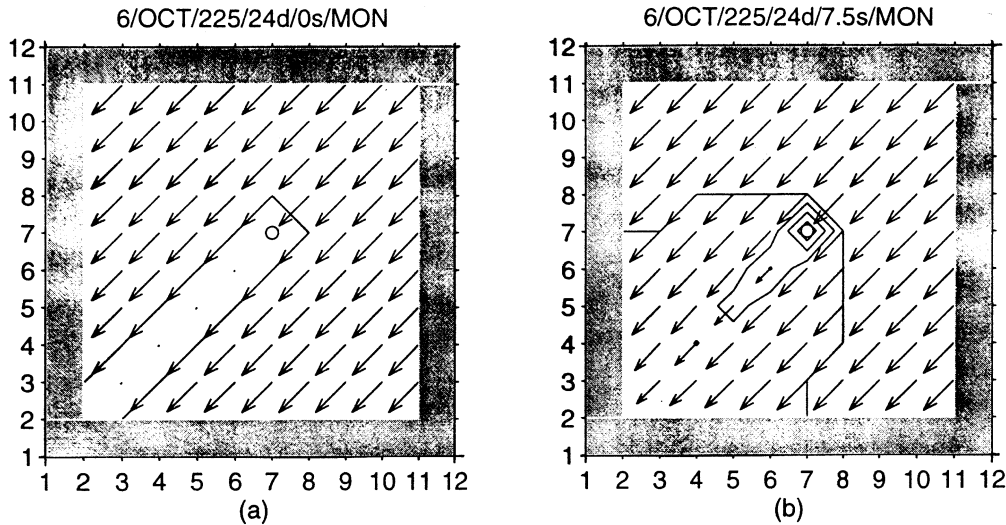


Fig. 9. – Advection past an island, represented by the isolated circle. See table I for details on the single test. The wave height isolines are spaced at 25% of the undisturbed value. a) Mono-frequency, uni-directional spectrum, b) as a), but with directional shift.

In general the O scheme is more sensitive to the problem, for the larger (eight instead of four) number of possible directions. The case of 24 spectral directions (equally spaced by  $15^\circ$ ) is shown in fig. 8c. As in the 12-direction case, the solution is a shift of the direction of half the directional resolution (in this case  $7.5^\circ$ ), as shown in panel 8d.

The application of the direction scheme of panels 8c and d is shown in fig. 9. Figure 9a shows the classical shadowing of the isolated island for waves from  $45^\circ$  and O scheme. As mentioned, the shift of the considered directions by  $7.5^\circ$  eliminates the problem, providing the more realistic results of panel 9b.

## 5. – Conclusions

To overcome numerical energy loss experienced by the first order upwind advection scheme when waves move parallel to and close to the coast, we have introduced an alternative scheme that, instead of along four directions, propagates energy along eight directions. This new scheme is potentially beneficial in areas with a complicated coastal shape and with scattered islands, where a “traditional” first order upwind advection scheme may lead to unrealistic over- or under-shadowing effects. To compare the performance of the two schemes, we have analyzed their behaviour in different conditions and with several different coastline geometries. The two schemes we have considered can behave quite differently with identical coastlines.

In the presence of a coastal corner the strong lateral diffusion intrinsic in the Q scheme causes a strong diffusion in the shadowed area (fig.4). This leads to an undesired numerical “false diffraction”, *i.e.* the wave field is numerically pivoted around the edge of an obstacle. In addition, the unphysical meaning of the results is

stressed by the fact that, contrary to actual diffraction effects, the wave direction in the shadowed area is the same of the incoming wave direction. In practice, this problem is smoothed by the directional energy distribution, which leads to a more realistic direction in the shadow area. However, it maintains a false diffraction pattern which extends from the corner point far beyond the few wavelengths we expect from realistic diffraction patterns corresponding to the problem layout of fig. 4.

The O scheme allows more energy to flow through narrow gaps, because of its capability to transfer the energy along the diagonals of the single mesh element. This becomes critical when the land reduces to a sequence of oblique points (fig. 6). In this case, while O allows a flow through the “islands”, Q sees the obstacle as a continuous coast and no energy flow is possible.

The relevant conclusion is that, in representing coastal geometry in a grid, we need to consider which advection system is used, its characteristics, and to design the grid so that the model results do reproduce the natural observations. For example, if we deal with a protruding oblique peninsula and we are using the O scheme, we need to use a double line of land points, as in layout 4 of fig. 3. Otherwise the model would interpret the protruding part as islands and let energy flow through, as in fig. 6b. Turning the problem around, to reproduce the results we expect in nature, the computational grid must be designed according to the advection scheme used in the wave model.

The case of an isolated island leads us to consider the transverse (with respect to the wave direction) properties of the O and Q schemes. Energy flowing along one of the main advection directions remains there, with no transversal diffusion. In this case the shadow of an island extends indefinitely along the grid. In practice, this effect is smoothed by the directional spreading, so that a tendency to fill the gap behind the islands does exist. However, especially in case of swell, the shadow may turn out to be quite long and unrealistic. The problem can be overcome by shifting the array of directions so that no one of them coincides with the directions of advection, as showed in fig. 8. The effect of the shift depends on the number of directions and on the advection scheme.

If a spherical co-ordinate system is used instead of a Cartesian one, a long shadowing effect is possible only along the meridians and the equator. This is because in these cases the energy flux is divergence free, *i.e.* it does not experience any apparent refraction related to the choice of the co-ordinate system; see Groves and Melcer (1961). In other cases the energy flow direction turns gradually away from the original one, preventing an extended shadowing effect. The bending will be southwards or northwards, depending on being in the Northern or Southern hemisphere.

As a final remark we recommend a careful check of results to spot unrealistic over- or under-shadowing effects in the proximity of islands, straits, peninsulas and “corner points” which, if disregarded, may lead to unrealistic results. To optimize the agreement between the numerical results and what we find in nature, it may be worth adopting an apparently unrealistic grid and/or shifting the directions along which the spectrum is discretized.

\* \* \*

This work was supported by the Human Capital Mobility Program of the European Union (contract No. ERB CHB GCT 930331) and by the MAST project Eurowaves (contract No. MAST3-CT97-0109). Thanks are due to R. FLATHER, J. C. HARGREAVES and to W. LUO who contributed with many helpful discussions and support.

## REFERENCES

- BIDLOT J., HANSEN B. and JANSSEN P. A. E. M., *Modifications to the ECMWF WAM code*, ECMWF Tech. Mem. No. 232 (1997) pp. 28.
- CAVALERI L. and SCLAVO M., *Characteristics of quadrant and octant advection schemes in wave models*, *Coast. Eng.*, **34** (1998) 221-242.
- GROVES G. W. and MELCER J., *On the propagation of ocean waves on a sphere*, *Geof. Int.*, **8** (1961) 77-93.
- KOMEN G. J., CAVALERI L., DONELAN M., HASSELMANN K., HASSELMANN S. and JANSSEN P. A. E. M., *Dynamics and Modelling of Ocean Waves* (Cambridge University Press) 1994, pp. 522.
- LUO W. and SCLAVO M., *Improvement of the Third Generation WAM Model (Cycle 4) for Applications in Nearshore Regions*, Proudman Oceanographic Laboratory report No. 116, 1997.
- RIS R. C., *Spectral modelling of wind waves in coastal areas. Communications on Hydraulic and Geotechnical Engineering*, Delft University of Technology, Rep. No. 97/4 (1997), pp. 158.
- RIS R. C., HOLTHUIJSEN L. H. and BOOIJ N., *A spectral model for waves in the near shore zone. Proceedings of the XXIV Coastal Engineering Conference*, Kobe, Japan (1994), pp. 68-78.
- TOLMAN H. L., *The numerical model WAVEWATCH: a third generation model for the hindcasting of wind waves on tides in shelf seas*, *Communications on Hydraulic and Geotechnical Engineering*, Delft University of Technology, Rep. No. 89/2 (1989), pp. 72.
- TOLMAN H. L., *A third-generation model for wind waves on slowly varying, unsteady, and inhomogeneous depths and currents*, *J. Phys. Ocean.*, **21** (1991) 782-794.
- WAMDI GROUP: HASSELMANN S., HASSELMANN K., BAUER E., JANSSEN P. A. E. M., KOMEN G. J., BERTOTTI L., LIONELLO L., GUILLAUME A., CARDONE V. C., GREENWOOD J. A., REISTAD M., ZAMBRESKY L. and EWING J. A., *The WAM model - A third generation ocean wave prediction model*, *J. Phys. Ocean.*, **18** (1998) 1775-1810.